



Global glacier change in the 21st century: Every increase in temperature matters

Rounce, D. R., Hock, R., Maussion, F., Hugonnet, R., Kochtitzky, W., Huss, M., Berthier, E., Brinkerhoff, D. J., Compagno, L., Copland, L., Farinotti, D., Menounos, B., & McNabb, R. (2023). Global glacier change in the 21st century: Every increase in temperature matters. *Science*, 379(6627), 78-83. Advance online publication. <https://doi.org/10.1126/science.abo1324>

[Link to publication record in Ulster University Research Portal](#)

Published in:
Science

Publication Status:
Published online: 05/01/2023

DOI:
[10.1126/science.abo1324](https://doi.org/10.1126/science.abo1324)

Document Version
Author Accepted version

General rights

Copyright for the publications made accessible via Ulster University's Research Portal is retained by the author(s) and / or other copyright owners and it is a condition of accessing these publications that users recognise and abide by the legal requirements associated with these rights.

Take down policy

The Research Portal is Ulster University's institutional repository that provides access to Ulster's research outputs. Every effort has been made to ensure that content in the Research Portal does not infringe any person's rights, or applicable UK laws. If you discover content in the Research Portal that you believe breaches copyright or violates any law, please contact pure-support@ulster.ac.uk.

Title: Global glacier change in the 21st century: Every increase in temperature matters

Authors: David R. Rounce^{1,2*}, Fabien Maussion³, Regine Hock^{4,2}, Romain Hugonnet^{5,6,7}, William Kochtitzky⁸, Matthias Huss^{5,6,9}, Etienne Berthier⁷, Douglas Brinkerhoff¹⁰, Loris Compagno^{5,6}, Luke Copland⁸, Daniel Farinotti^{5,6}, Brian Menounos^{11,12}, Robert W. McNabb¹³

Affiliations:

¹Department of Department of Civil & Environmental Engineering, Carnegie Mellon University; Pittsburgh, PA, USA

²Geophysical Institute, University of Alaska Fairbanks; Fairbanks, AK, USA

³Department of Atmospheric and Cryospheric Sciences, University of Innsbruck; Innsbruck, Austria

⁴Department of Geosciences, University of Oslo; Oslo, Norway

⁵Laboratory of Hydraulics, Hydrology and Glaciology (VAW), ETH Zürich; Zurich, Switzerland

⁶Swiss Federal Institute for Forest, Snow and Landscape Research (WSL); Birmensdorf, Switzerland

⁷LEGOS, Université de Toulouse, CNES, CNRS, IRD, UPS; Toulouse, France

⁸Department of Geography, Environment and Geomatics, University of Ottawa; Ottawa, Ontario, Canada

⁹Department of Geosciences, University of Fribourg; Fribourg, Switzerland

¹⁰Department of Computer Science, University of Montana; Missoula, MT, USA

¹¹Geography Earth and Environmental Sciences, University of Northern British Columbia; Prince George, BC, Canada

¹²Hakai Institute; Campbell River, BC, Canada

¹³School of Geography and Environmental Sciences, Ulster University; Coleraine, UK

*Corresponding author. Email: drounce@cmu.edu

Abstract: Glacier mass loss impacts sea-level rise, water resources, and hazards. We present global glacier projections, excluding the ice sheets, for Shared Socioeconomic Pathways calibrated with data for each glacier. Glaciers are projected to lose $26\pm 6\%$ ($+1.5^\circ\text{C}$) to $41\pm 11\%$ ($+4^\circ\text{C}$) of their mass by 2100, relative to 2015, for global temperature change scenarios. This corresponds to 90 ± 26 to 154 ± 44 mm sea level equivalent and causes $49\pm 9\%$ to $83\pm 7\%$ of glaciers to disappear. Mass loss is linearly related to temperature increase, thus reductions in temperature increase reduce mass loss. Based on climate pledges from the Conference of Parties (COP-26) global mean temperature is projected to increase by $+2.7^\circ\text{C}$, which would lead to a sea-level contribution of 115 ± 40 mm and cause widespread deglaciation in most mid-latitude regions.

One-Sentence Summary: Projected glacier mass loss stresses urgency of limiting global warming to reduce sea-level rise and widespread deglaciation.

Main Text: Glaciers, here referring to all glacial land ice excluding the Greenland and Antarctic ice sheets, are responsible for $21\pm 3\%$ of sea-level rise from 2000-2019, contributing 0.74 ± 0.04 mm sea level equivalent (SLE) yr^{-1} (1). Projections suggest this contribution could increase to 2.5 mm SLE yr^{-1} by 2100 (2). Glaciers are also a critical water resource for ~ 1.9 billion people (3), and projected losses will alter water availability impacting annual and seasonal runoff (4). Glacier-related hazards, including glacier outburst floods, are also expected to change in frequency and magnitude over the next century due to mass loss (5). Projecting the magnitude, spatial pattern and timing of glacier mass loss is therefore essential to support climate adaptation and mitigation efforts for communities ranging from the coast to the high mountains.

Previous projections of glacier mass loss from the Glacier Model Intercomparison Project (GlacierMIP) (2) estimated glacier contribution to sea-level rise for ensembles of Representative Concentration Pathways (RCPs), and results were extended to Shared Socioeconomic Pathways (SSPs) using statistical models of these simulations (6). GlacierMIP provided these projections at regional scales based on simulations from 11 glacier evolution models that varied with respect to the complexity of model physics, simulated physical processes, model calibration, spatial resolution, and modeling domain. Calibration data varied from in-situ measurements of less than 300 of the world's more than 215,000 glaciers to regional geodetic and/or gravimetric mass balance observations. Furthermore, only one global model simulated glacier dynamics using a flowline model (7), while all others relied on empirical volume-area scaling or parameterizations of mass redistribution; only one model accounted for frontal ablation (i.e., the sum of iceberg calving and submarine melt) of marine-terminating glaciers (8), while all others treated any glacier as land-terminating; and no global model accounted for debris cover. Existing multi-model projections (2, 6, 9) are thus limited to regional scales and neglect key physical processes controlling glacier mass loss.

Here we produce a set of global glacier projections for every individual glacier on Earth for SSPs from 2015 to 2100 by leveraging global glacier mass balance data (1) and nearly-global frontal ablation data (10–13). To provide policy-relevant scenarios, our projections are grouped based on mean global temperature increases by the end of the 21st century compared to pre-industrial levels to explicitly link differences in glacier mass loss, sea-level rise, and the number of glaciers that vanish in response to changes in mean global temperature. Our glacier evolution model, a hybrid of the Python Glacier Evolution Model (PyGEM) (14, 15) and Open Global Glacier Model (OGGM) (7), enables us to produce global glacier projections that explicitly account for glacier dynamics using a flowline model (7) based on the shallow-ice approximation (16); the effects of debris thickness on sub-debris melt rates (17), and frontal ablation (8). Our estimates of glacier contribution to sea-level rise also account for the roughly 15% of ice from marine-terminating glaciers that is already below sea level (18). Projections are also reported for SSPs and RCPs to highlight differences compared to previous studies.

Projections of policy-relevant scenarios

The Paris Agreement, adopted in 2015 by 195 countries, agreed to keep the increase in global mean temperature by the end of the 21st century relative to pre-industrial levels below 2°C , and that efforts should be made to limit the temperature change to 1.5°C . This target was kept alive in the Glasgow Agreement adopted by the Conference of the Parties (COP26) in 2021. To evaluate the sensitivity of glaciers to global mean temperature increases, the glacier projections are aggregated into $+1.5^\circ\text{C}$, $+2^\circ\text{C}$, $+3^\circ\text{C}$, and $+4^\circ\text{C}$ temperature change scenarios by 2100 relative to pre-industrial levels (Fig. 1).

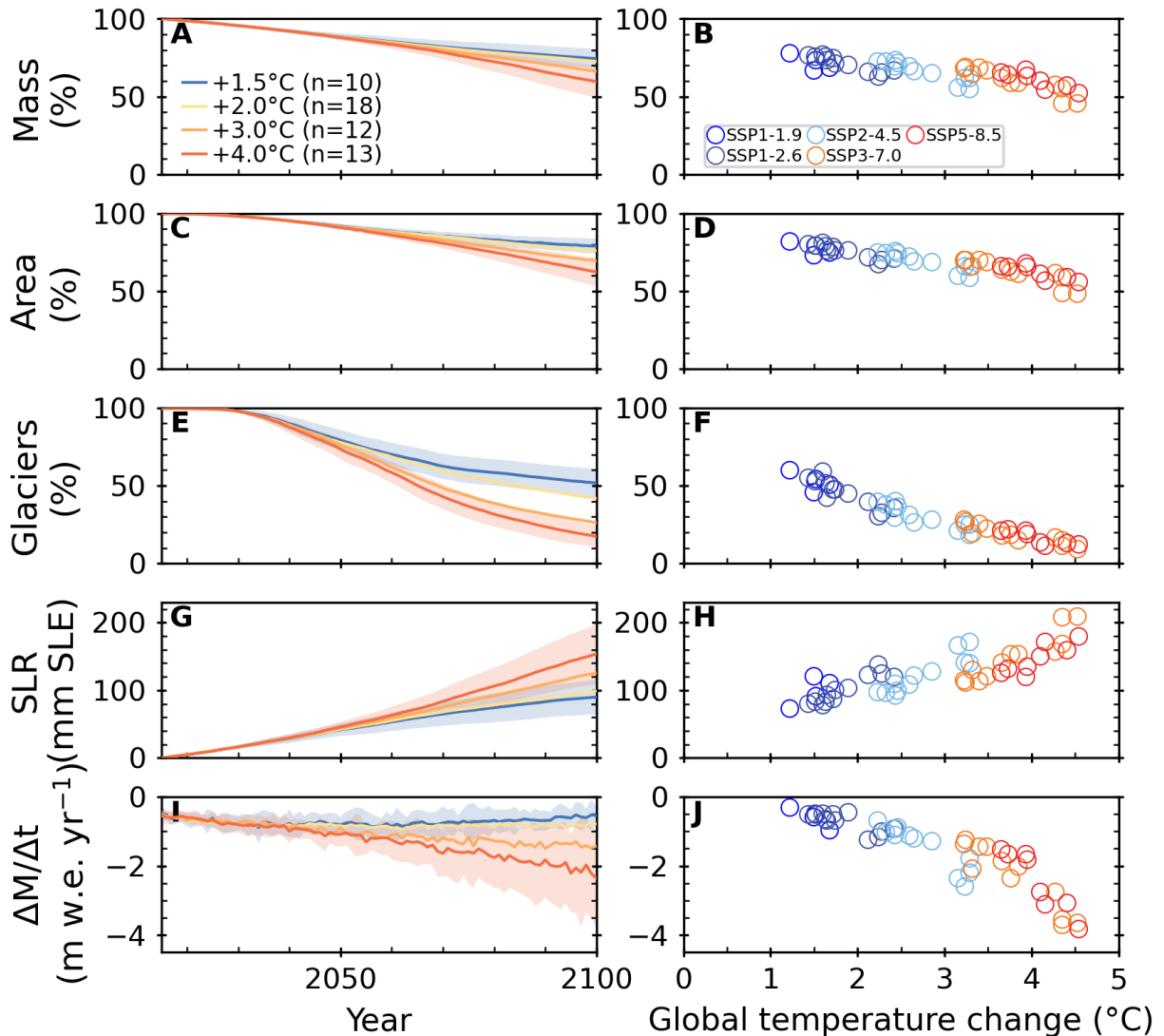


Fig. 1. Projected global glacier changes for scenarios of global mean temperature change.

(A, B) Mass remaining, (C, D) area remaining, (E, F) glaciers remaining, (G, H) sea-level rise (SLR) contributed from glaciers, and (I, J) area-averaged mass change rate for all glaciers globally. Projections are shown from 2015 to 2100 (left panels), and at 2100 (right panels). Values in (A) - (H) are relative to 2015. Colors depict the global mean temperature change scenarios (left panels) and the SSPs corresponding to the global temperature changes (right panels). The number (n) of glacier projections with different GCMs and SSPs that fall into each temperature change scenario is shown in the legend. Lines (left panels) show the ensemble median and shading indicates the 95% confidence interval for each temperature change scenario.

Globally, glaciers are projected to lose $26 \pm 6\%$ ($+1.5^\circ\text{C}$) to $41 \pm 11\%$ ($+4^\circ\text{C}$) of their mass by 2100, relative to 2015 (ensemble median \pm 95% confidence interval). This mass loss would increase mean sea level by 90 ± 26 mm SLE under the $+1.5^\circ\text{C}$ scenario and 99 ± 31 mm SLE under the $+2^\circ\text{C}$ scenario. The higher temperature change scenarios of $+3^\circ\text{C}$ and $+4^\circ\text{C}$ lead to

contributions of 125 ± 39 and 154 ± 44 mm SLE, respectively, highlighting a 71% increase between the $+1.5^\circ\text{C}$ and $+4^\circ\text{C}$ scenarios.

The rate of sea-level rise from glacier losses near the end of the 21st century ranges from 0.70 ± 0.45 to 2.23 ± 1.08 mm SLE yr^{-1} depending on the temperature change scenario (Fig. S1). For $+1.5^\circ\text{C}$, the rate of sea-level rise peaks at 1.29 ± 0.59 mm SLE yr^{-1} around 2035 and declines thereafter, while the rate for $+4^\circ\text{C}$ steadily increases for the remainder of this century. Similar trends are observed in the area-averaged mass loss rate, where the maximum loss rate of 0.82 ± 0.36 m water equivalent (w.e.) yr^{-1} occurs around 2035 before diminishing to 0.59 ± 0.34 m w.e. yr^{-1} at the end of the century for the $+1.5^\circ\text{C}$ scenario; the mass loss rate continuously increases to 2.02 ± 1.30 m w.e. yr^{-1} by the end of the century for the $+4^\circ\text{C}$ scenario (Fig. 1I). Even if the global mean temperature change is limited to $+1.5^\circ\text{C}$, we estimate that $104,000\pm 20,000$ glaciers (49 \pm 9% of the total inventoried) will disappear by 2100 and at least half of those will be lost prior to 2050 (Fig. 1E). Most of the glaciers projected to disappear are smaller than 1 km² (Fig. 2), but despite their small size their disappearance may still negatively impact local hydrology, tourism, glacier hazards, and cultural values (19). Glaciers projected to disappear represent 2-8% of the glacier contribution to sea-level rise depending on the temperature change scenario.

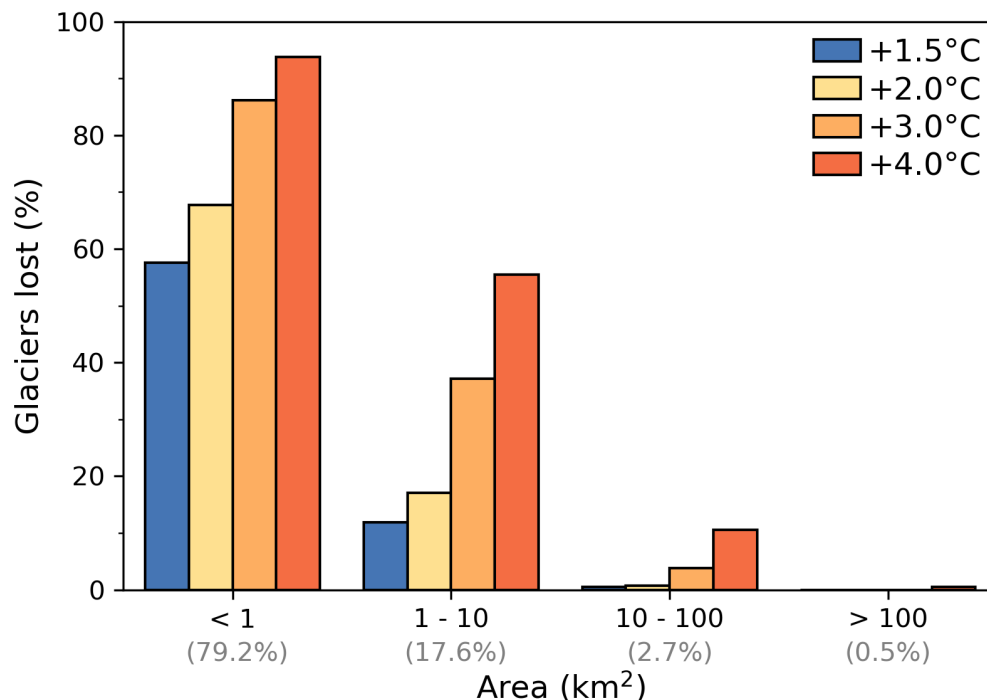


Fig. 2. Percent of glaciers projected to vanish between 2015 and 2100 for global temperature change scenarios sorted by size. The glaciers are binned according to their initial glacier area and the numbers below each bin (shown in grey) refer to the percentage of the total number of glaciers in 2015 in each bin.

Regional mass changes

Regional variations exist in the glacier mass change projections (Fig. 3). Alaska is the largest regional contributor to global mean sea-level rise from 2015 to 2100 (Fig. S2), peaking at 0.33 to 0.44 mm SLE yr^{-1} between 2030 and 2060 depending on the temperature change scenario, before

decreasing to 0.13 to 0.28 mm SLE yr⁻¹ by 2100 (Fig. S1). Greenland Periphery, Antarctic and Subantarctic, Arctic Canada North, and Arctic Canada South contribute 12, 10, 10, and 9% to projected sea-level rise, respectively. Collectively, these five regions account for 60-65% of the total glacier contribution to sea-level rise. For Greenland Periphery, Arctic Canada North, and Arctic Canada South, the rate of the contribution to sea-level rise is almost insensitive to temperature change below +2°C, but steadily increases through 2100 for the other temperature change scenarios. For the +3°C and +4°C scenarios, the rate of sea-level rise from Greenland Periphery, Antarctic and Subantarctic, and Arctic Canada North each nearly equal or exceed Alaska near the end of the century, with Antarctic and Subantarctic and Arctic Canada North accelerating throughout the 21st century. Since projected glacier mass loss includes both the instantaneous response of glaciers to climate forcing and the delayed response based on the extent of disequilibrium to longer-term climatic conditions (e.g., 20), these regions with large glaciers will continue losing mass beyond 2100, especially for higher temperature change scenarios.

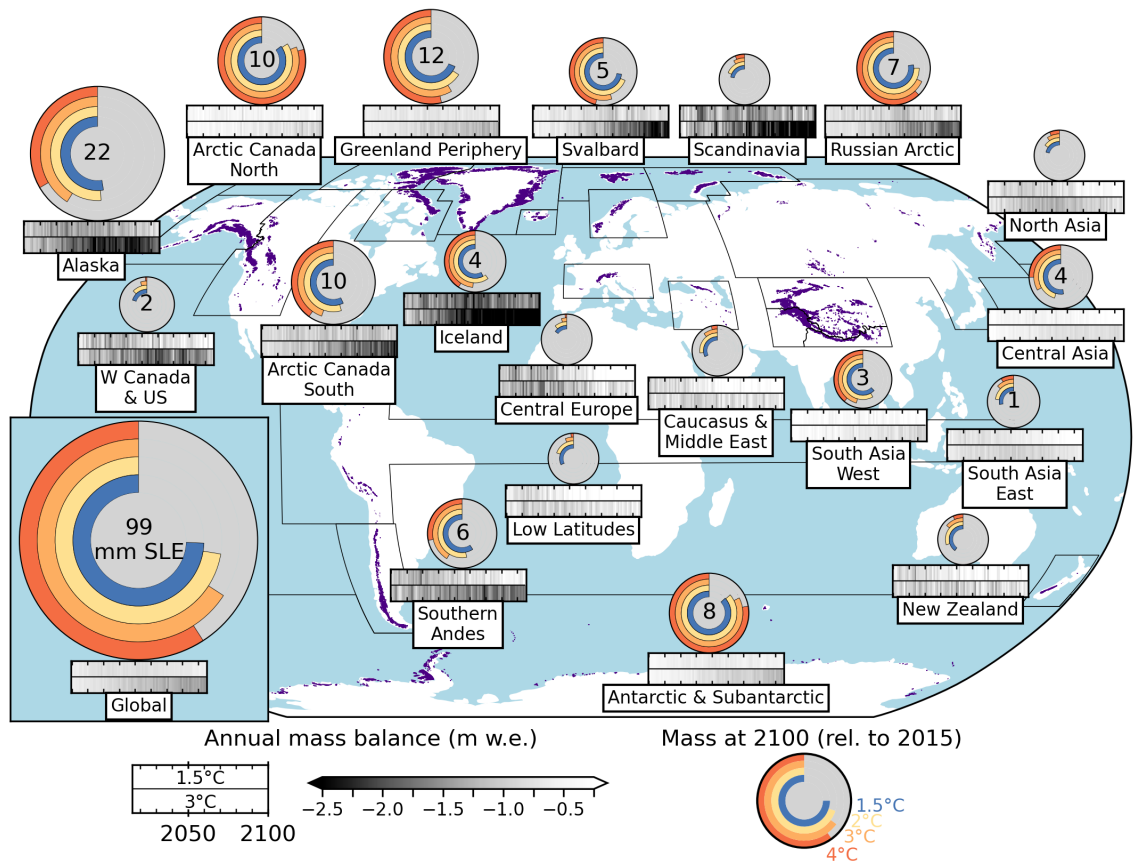


Fig. 3. Regional glacier mass change and contributions to sea level rise from 2015 to 2100. Discs show global and regional projections of glacier mass remaining by 2100, relative to 2015, for global mean temperature change scenarios. Discs are scaled based on each region's contribution to global mean sea level rise from 2015 to 2100 for the +2°C scenario by 2100 relative to pre-industrial levels and nested rings are colored by temperature change scenarios showing normalized mass remaining in 2100. Regional sea level rise contributions larger than 1 mm SLE for the +2°C scenario are printed in the center of the pie chart. The horizontal bars show time series of area-averaged annual mass balance from 2015 to 2100 for +1.5°C (top) and

+3°C (bottom) scenarios. The colorbar is saturated at -2.5 m w.e., but minimum annual values reach -4.2 m w.e. in Scandinavia. Time series of regional relative mass change and regional area-averaged mass change are shown in Figs. S3-4.

5 Western Canada and US, South Asia East, Scandinavia, North Asia, Central Europe, Low
Latitudes, Caucasus and Middle East, and New Zealand, are projected to lose 60-100% of their
glacier mass depending on the temperature change scenario (Figs. 3, S3). The temperature
change scenario thus has a major impact on the mass loss, in some cases determining whether the
complete deglaciation of regions occurs by the end of the 21st century. While these regions are
10 not significant contributors to sea-level rise, people in these regions will need to adapt to changes
in seasonal and annual runoff as the additional water provided by glacier net mass loss will
decline before 2050 as the glaciers retreat (Figs. S5-8). In High Mountain Asia, the timing of
maximum rates of mass loss varies, with South Asia East peaking between 2025-2030, Central
Asia between 2035-2055, and South Asia West between 2050-2075, depending on the
15 temperature change scenario.

Regional sensitivity to temperature change

The sensitivity of the glacierized regions to changes in global mean temperature depends on the
region's current glacier mass and mass change rates; regional temperature anomalies relative to
the global mean (Fig. 4), such as those associated with Arctic amplification (21); the climatic
20 setting (maritime versus continental) and sensitivity to precipitation falling as rain instead of
snow; and elevation feedbacks due to different types of glaciers (e.g., ice caps versus valley
glaciers) (22). Projected mass loss is linearly related to global mean temperature increase,
especially for larger glacierized regions, consistent with a recent study (6). This strong
relationship highlights that every fraction of a degree of temperature increase significantly
25 impacts glacier mass loss. The smallest glacierized regions by mass, including Central Europe,
Scandinavia, Caucasus and Middle East, North Asia, Western Canada and US, Low Latitudes,
and New Zealand, will experience near-complete deglaciation around +3°C. These regions are
thus highly sensitive to global mean temperature increases between 1.5 and 3°C and have a
nonlinear response above 3°C of warming.

30 The strength of the linear relationship varies among regions, which reflects differences in the
regional temperature anomalies from the ensemble of GCMs (evident from the larger standard
deviations given in Figs. 4, S9). Regions like Alaska, Southern Andes, and Central Asia have
less scatter indicating less variation in the regional temperature anomaly and thereby a more
consistent response to climate forcing (mean $R^2=0.78$). Other regions like the Russian Arctic,
35 Svalbard, and Iceland have more variation in the regional temperature anomaly and thus a
weaker linear relationship (mean $R^2=0.50$) as well as significant variations in projected
precipitation (Fig. S10). Future work using regional climate projections may better resolve high-
mountain climatic conditions and refine projections in these regions (e.g., 22).

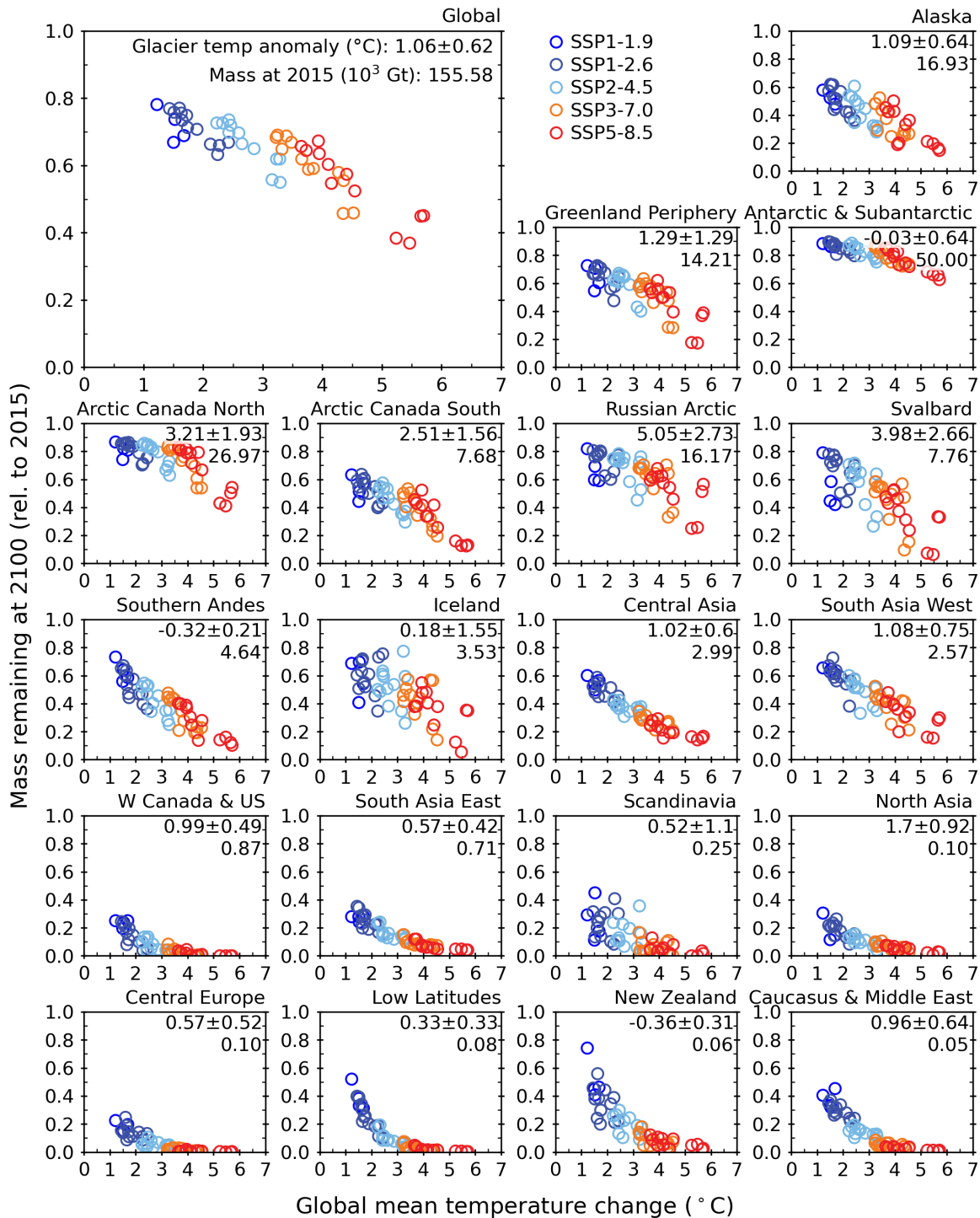


Fig. 4. Fraction of global and regional mass remaining at 2100, relative to 2015, as a function of global mean temperature change by 2100 relative to pre-industrial levels. Each marker represents results from one GCM and SSP. Numbers indicate global and regional median temperature anomalies (\pm standard deviation) ($^{\circ}\text{C}$) over glacierized areas, relative to the mean temperature change over the entire globe at 2100 relative to pre-industrial levels, for all GCMs and scenarios. Negative values indicate that some regions warm less than the global average. Regions are ordered by their total mass loss.

Spatially resolved projections at glacier scale

Our projections reveal notable spatial variations in glacier mass loss at the local scale for the temperature change scenarios (Fig. 5). All regions are projected to lose some glaciers completely, primarily smaller ice masses, with the higher temperature change scenarios revealing significantly more mass loss and the deglaciation of greater areas (Figs. S11-13). While Central Europe, Caucasus and Middle East, North Asia, and Western Canada and US are projected to experience widespread deglaciation for the +2°C scenario, our results also reveal where remaining glaciers will be concentrated at the end of this century. Besides the Karakoram and Kunlun in High Mountain Asia, the remaining mass is primarily located in southeastern Alaska, Arctic Canada North, Svalbard, the Russian Arctic, Greenland Periphery, and Antarctic and Subantarctic. Given that these regions comprise a significant number of marine-terminating glaciers, accounting for frontal ablation is critical over the next century and beyond.

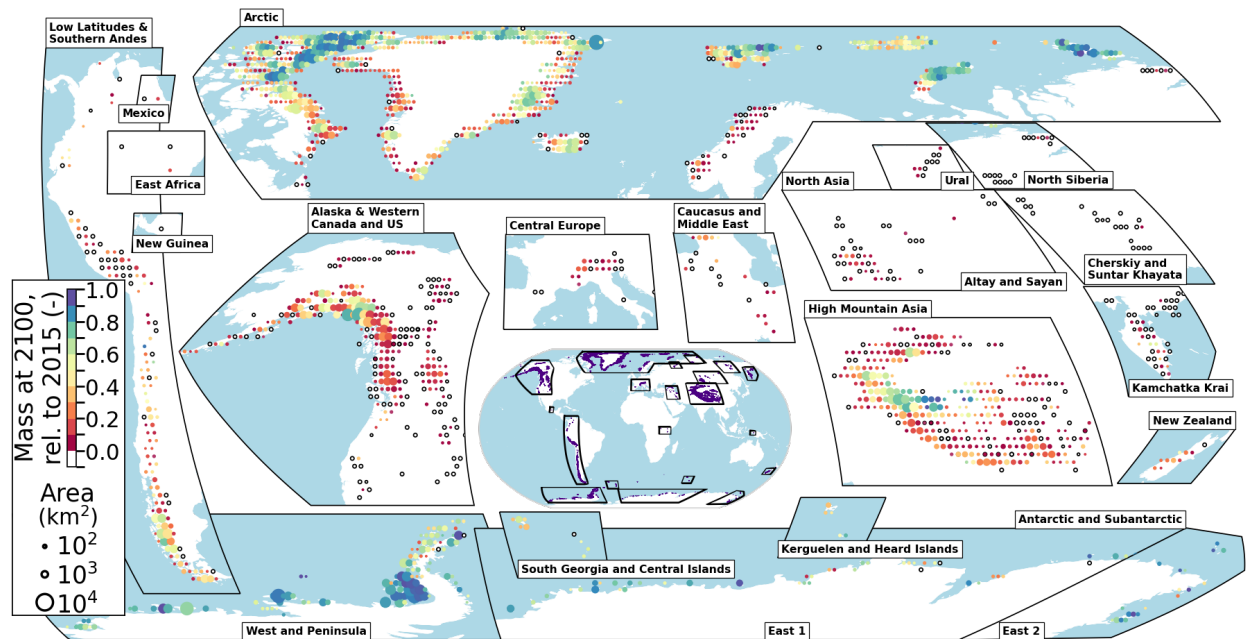


Fig. 5. Spatial distribution of glacier mass remaining by 2100 for the +2°C scenario. The ensemble median glacier mass remaining by 2100 (relative to 2015) for the +2°C (above pre-industrial levels) global mean temperature change scenario. Tiles are aggregated by 1°x1° below 60° latitude, 2°x1° between 60° and 74° latitude and 2°x2° above 74° latitude to represent approximately 10,000 km² each. Circles are scaled based on simulated glacierized area in 2015 and are colored by normalized mass remaining. Regions that have experienced complete deglaciation by 2100 are shown in white and outlined in black. High Mountain Asia refers to Central Asia, South Asia West, and South Asia East. Specific subregions are noted by labels on the bottom of inset figures. Additional temperature change scenarios (+1.5, +3, and +4 °C) are shown in Figs. S11-13.

Importance of marine-terminating glaciers

Marine-terminating glaciers represent 40% of the total present-day global glacier area (23), and this percentage reaches 99% for the Antarctic and Subantarctic region. Most previous global glacier projections do not explicitly account for frontal ablation (2), instead implicitly accounting for it by increasing melt rates, thereby poorly accounting for dynamical feedbacks associated

with the glacier's evolution. Our model couples a frontal ablation parameterization with a flowline model and uses a state-of-the-art calibration scheme, ice thickness inversion method, and geodetic mass balance and frontal ablation calibration data (see Methods). This enables us to project changes of individual marine-terminating glaciers and determine if and when they become land-terminating (Fig. S14). Separate simulations including and excluding frontal ablation, with model parameters calibrated separately for both, are used to quantify its impact on projections.

Counterintuitively, we estimate that accounting for frontal ablation reduces the glacier contribution to mean sea-level rise from 2015-2100 by 2% for each temperature change scenario, compared to models not including frontal ablation. From 2015-2100 frontal ablation accounts for $91 \pm 10 \text{ Gt yr}^{-1}$ ($+1.5^\circ\text{C}$) to $88 \pm 8 \text{ Gt yr}^{-1}$ ($+4^\circ\text{C}$) of the total glacier mass loss globally (Figs. S15-18). For the $+2^\circ\text{C}$ scenario, the rate of mass loss due to frontal ablation diminishes over the century from $115 \pm 11 \text{ Gt yr}^{-1}$ in 2000-2020 to $75 \pm 8 \text{ Gt yr}^{-1}$ in 2080-2100. Diminished mass losses from frontal ablation of marine-terminating glaciers reflect their thinning, retreat onto land (44-57% of all marine-terminating glaciers) (Fig. S19), and reduced ice flux into the ocean, which occurs for all temperature change scenarios. The relative contribution of frontal ablation to total ablation (i.e., frontal ablation plus melt) ranges from 11% ($+1.5^\circ\text{C}$) to 8% ($+4^\circ\text{C}$) for 2015-2100, diminishing for higher temperature change scenarios due to increases in melt. Regionally, the relative contribution of frontal ablation for all temperature change scenarios is greatest in Antarctic and Subantarctic (34%), the Russian Arctic (34%), and Svalbard (17%) (Figs. S15-18).

The impact of not accounting for frontal ablation on relative mass loss (i.e., glacier mass loss by 2100 relative to 2015) varies greatly by region (Fig. S20). For Alaska and Svalbard, excluding frontal ablation increases relative mass loss at 2100 by 2-8% depending on the temperature change scenario. The Russian Arctic varies from a 2% reduction ($+1.5^\circ\text{C}$) to a 5% increase ($+4^\circ\text{C}$). Arctic Canada, Greenland Periphery, and Southern Andes see almost no difference ($\pm 2\%$), and Antarctic/Subantarctic sees a 0-2% decrease in relative mass loss. These results highlight the complex response of marine-terminating glaciers, which are dependent on the frontal ablation rate, glacier geometry, and surface mass balance. In the Antarctic and Subantarctic, we find excluding frontal ablation decreases the regional relative mass loss, since mass loss due to frontal ablation is greater than the increased melt when frontal ablation is excluded. Conversely, in Alaska and Svalbard, the regional relative mass loss increases when frontal ablation is excluded, since mass loss due to frontal ablation is less than the increased melt when frontal ablation is excluded.

Importance of debris-covered glaciers

Debris currently covers 4-7% of the global glacier area (24, 25). A thin layer of debris ($< 3\text{-}5 \text{ cm}$) enhances surface melt, while a thick layer insulates the underlying ice and reduces melt (26). The spatial distribution of debris thickness can cause debris-covered glaciers to develop stagnant glacier tongues and eventually separate from the active part of the glacier (27, 28). Our representation of debris and glacier dynamics enables us to simulate these complex feedbacks, including reduced melt at glacier termini where debris is thick (Fig. S21). We thus produce a set of global glacier projections that account for debris and compare these to separate simulations that exclude debris (i.e., treat the debris as clean ice) to quantify the insulating effect that debris has on glacier projections.

The impact of debris on relative mass loss varies greatly spatially and temporally (Fig. S22) with the most significant differences occurring in the mid-century in New Zealand and South Asia

East. In these regions, the insulating effect of debris reduces net mass loss by 9-13% depending on the temperature change scenario, although the differences are less than 5% by 2100. Alaska, the largest region by mass with considerable debris cover (>5% by area), sees a reduction of 5% around 2060 and 3% by 2100. Other regions with considerable debris cover (> 5% by area), including Western Canada and US, Central Europe, Caucasus and Middle East, and Low Latitudes, see a reduction in mass loss of less than 5% in the mid-century and no difference ($\pm 1\%$) by 2100. The inclusion of debris thus delays mass loss over the century, especially at local scales, but has little impact on sea-level rise and the number of glaciers lost by 2100. The limited impact in most regions shows that the insulating effect of debris is unable to offset the increased melt for the various temperature change scenarios.

Comparison with previous projections

For comparison with recent multi-model studies (2, 6), we also report our projections for the RCPs and SSPs. Our global projections of glacier contribution to sea-level rise for 2015-2100 range from 90 ± 36 mm SLE (RCP2.6) to 163 ± 53 mm SLE (RCP8.5) and 98 ± 38 mm SLE (SSP1-2.6) to 166 ± 83 mm SLE (SSP5-8.5), respectively (Table 1). These projections include a correction (reduction) of 17 to 24 mm SLE, which accounts for the mass loss of ice from marine-terminating glaciers that is below sea level and therefore will not contribute to global mean sea-level rise; an important difference compared to the current multi-model studies (2, 6) which do not account for this. Even with this correction, for the low emissions scenarios our RCP2.6 projections are 11 mm SLE (14%) greater than Marzeion et al. (2), and our SSP1-2.6 projections are 18 mm SLE (23%) greater than Edwards et al. (6). For the mid-range (RCP4.5 and SSP2-4.5) and high (RCP8.5, SSP5-8.5) emissions scenarios, our projections are within ± 7 mm SLE of than both studies.

Table 1. Projected global glacier mass loss and glacier contribution to sea-level rise. Results are shown for RCP and SSP scenarios at 2100, relative to 2015, from this study and recent multi-model studies (2, 6). ‘Uncorrected’ refers to projections that assume mass losses below sea level contribute to sea-level rise, consistent with assumptions in recent multi-model studies. Note that uncertainty associated with the multi-model studies is expressed as 90% confidence interval, while this study reports ensemble median and 95% confidence interval. Regional comparisons are shown in Tables S1-2.

Global glacier contribution to sea-level rise from 2015 to 2100 (mm SLE)						
Study	RCP2.6	RCP4.5	RCP8.5	SSP1-2.6	SSP2-4.5	SSP5-8.5
This study	90 ± 36	114 ± 44	163 ± 53	98 ± 38	116 ± 51	166 ± 83
This study (uncorrected)	106 ± 37	132 ± 47	187 ± 61	115 ± 42	135 ± 57	192 ± 97
Marzeion et al. (2)	79 ± 57	119 ± 66	159 ± 86	-	-	-
Edwards et al. (6)	-	-	-	80 ± 35	119 ± 39	159 ± 47
Global glacier mass loss, relative to 2015 (%)						
Study	RCP2.6	RCP4.5	RCP8.5	SSP1-2.6	SSP2-4.5	SSP5-8.5
This study	26 ± 8	31 ± 10	43 ± 13	28 ± 9	32 ± 12	44 ± 20
Marzeion et al. (2)	18 ± 13	27 ± 15	36 ± 20	-	-	-

Not correcting for the loss of ice below sea level, our projections of glacier contribution to sea-level rise from 2015-2100 are 11-44% greater than these multi-model estimates (2, 6) for all emission scenarios. We attribute these differences to the global mass balance data we used for calibration, which include an accelerated trend in mass loss from 2000-2020 (1), as well as the improved representation of physical processes in our model.

Globally, we predict glaciers will lose $26\pm 8\%$ (RCP2.6) to $43\pm 13\%$ (RCP8.5) and $28\pm 9\%$ (SSP1-2.6) to $44\pm 20\%$ (SSP5-8.5) of their mass by 2100, relative to 2015. Our projected relative mass losses are 4-8% greater than current multi-model estimates (2). Regionally, the most significant differences occur in Alaska, Arctic Canada South, South Asia East, and Southern Andes, where we predict 11-23% more relative mass loss (Table S1). In Alaska, we estimate 22% (RCP2.6) to 23% (RCP8.5) more relative mass loss compared to the multi-model estimates (2), and find a peak in the net mass loss rate in the middle of the century, in contrast to the peak net mass loss rate at the end of the century from the multi-model estimates (2).

A comparison of our projections from the ensembles of RCPs and SSPs used in this study reveals that glacier contribution to sea-level rise is 2-9% greater for SSPs than the corresponding RCPs. These differences are a result of the SSPs simulating greater temperature increases for the same radiative forcing as the RCPs (29, 30). Our ensembles reflect this higher warming sensitivity as our SSPs are on average 0.14-0.25°C warmer than their corresponding RCPs. Considering the high sensitivity of global and regional glacier mass loss to small temperature increases revealed by our study, the higher warming sensitivity of the SSPs will significantly impact the projected glacier contribution to sea-level rise as well as the number of glaciers anticipated to be lost.

Summary and way forward

Our projections reveal a strong linear relationship between global mean temperature increase and glacier mass loss, with the smallest glacierized regions having a nonlinear relationship beyond +3°C as they experience near complete deglaciation. This strong relationship at global and regional scales, highlights that every increase in temperature has significant consequences with respect to glacier contribution to sea-level rise, the loss of glaciers around the world, and changes to hydrology, ecology, and natural hazards. Regardless of the temperature change scenario, all regions will experience considerable deglaciation at local scales with roughly half of the world's glaciers, by number, projected to be lost by 2100 even if temperature increase is limited to +1.5°C. Based on the most recent climate pledges from COP26, global mean temperature is estimated to increase by +2.7°C (31), which would result in much greater glacier contribution to sea-level rise (115 ± 40 mm SLE) and the near complete deglaciation of entire regions including Central Europe, Western Canada and US, and New Zealand (Figs. 5, S11-13) compared to the Paris Agreement. The rapidly increasing glacier mass losses as global temperature increases beyond +1.5°C stresses the urgency of establishing more ambitious climate pledges to preserve these glacierized regions.

References

1. R. Hugonnet, R. McNabb, E. Berthier, B. Menounos, C. Nuth, L. Girod, D. Farinotti, M. Huss, I. Dussailant, F. Brun, A. Käab, Accelerated global glacier mass loss in the early twenty-first century. *Nature*. **592**, 726–731 (2021).

2. B. Marzeion, R. Hock, B. Anderson, A. Bliss, N. Champollion, K. Fujita, M. Huss, W. W. Immerzeel, P. Kraaijenbrink, J. H. Malles, F. Maussion, V. Radić, D. R. Rounce, A. Sakai, S. Shannon, R. van de Wal, H. Zekollari, Partitioning the Uncertainty of Ensemble Projections of Global Glacier Mass Change. *Earth's Future*. **8** (2020),
5 doi:10.1029/2019EF001470.
3. W. W. Immerzeel, A. F. Lutz, M. Andrade, A. Bahl, H. Biemans, T. Bolch, S. Hyde, S. Brumby, B. J. Davies, A. C. Elmore, A. Emmer, M. Feng, A. Fernández, U. Haritashya, J. S. Kargel, M. Koppes, P. D. A. Kraaijenbrink, A. v. Kulkarni, P. A. Mayewski, S. Nepal, P. Pacheco, T. H. Painter, F. Pellicciotti, H. Rajaram, S. Rupper, A. Sinisalo, A. B. Shrestha, D. Viviroli, Y. Wada, C. Xiao, T. Yao, J. E. M. Baillie, Importance and
10 vulnerability of the world's water towers. *Nature*. **577**, 364–369 (2020).
4. M. Huss, R. Hock, Global-scale hydrological response to future glacier mass loss. *Nature Climate Change*. **8**, 135–140 (2018).
5. S. Harrison, J. S. Kargel, C. Huggel, J. Reynolds, D. H. Shugar, R. A. Betts, A. Emmer, N. Glasser, U. K. Haritashya, J. Klimeš, L. Reinhardt, Y. Schaub, A. Wiltshire, D. Regmi, V. Vilimek, Climate change and the global pattern of moraine-dammed glacial lake
15 outburst floods. *Cryosphere*. **12**, 1195–1209 (2018).
6. T. L. Edwards, S. Nowicki, B. Marzeion, R. Hock, H. Goelzer, H. Seroussi, N. C. Jourdain, D. A. Slater, F. E. Turner, C. J. Smith, C. M. McKenna, E. Simon, A. Abe-
20 Ouchi, J. M. Gregory, E. Larour, W. H. Lipscomb, A. J. Payne, A. Shepherd, C. Agosta, P. Alexander, T. Albrecht, B. Anderson, X. Asay-Davis, A. Aschwanden, A. Barthel, A. Bliss, R. Calov, C. Chambers, N. Champollion, Y. Choi, R. Cullather, J. Cuzzone, C. Dumas, D. Felikson, X. Fettweis, K. Fujita, B. K. Galton-Fenzi, R. Gladstone, N. R. Golledge, R. Greve, T. Hattermann, M. J. Hoffman, A. Humbert, M. Huss, P. Huybrechts, W. Immerzeel, T. Kleiner, P. Kraaijenbrink, S. le clec'h, V. Lee, G. R. Leguy, C. M.
25 Little, D. P. Lowry, J. H. Malles, D. F. Martin, F. Maussion, M. Morlighem, J. F. O'Neill, I. Nias, F. Pattyn, T. Pelle, S. F. Price, A. Quiquet, V. Radić, R. Reese, D. R. Rounce, M. Rückamp, A. Sakai, C. Shafer, N. J. Schlegel, S. Shannon, R. S. Smith, F. Straneo, S. Sun, L. Tarasov, L. D. Trusel, J. van Breedam, R. van de Wal, M. van den Broeke, R.
30 Winkelmann, H. Zekollari, C. Zhao, T. Zhang, T. Zwinger, Projected land ice contributions to twenty-first-century sea level rise. *Nature*. **593**, 74–82 (2021).
7. F. Maussion, A. Butenko, N. Champollion, M. Dusch, J. Eis, K. Fourteau, P. Gregor, A. H. Jarosch, J. Landmann, F. Oesterle, B. Recinos, T. Rothenpieler, A. Vlug, C. T. Wild, B. Marzeion, The Open Global Glacier Model (OGGM) v1.1. *Geoscientific Model
35 Development*. **12**, 909–931 (2019).
8. M. Huss, R. Hock, A new model for global glacier change and sea-level rise. *Frontiers in Earth Science*. **3** (2015), doi:10.3389/feart.2015.00054.
9. R. Hock, A. Bliss, B. E. N. Marzeion, R. H. Giesen, Y. Hirabayashi, M. Huss, V. Radic, A. B. A. Slangen, GlacierMIP-A model intercomparison of global-scale glacier mass-
40 balance models and projections. *Journal of Glaciology*. **65**, 453–467 (2019).
10. B. Osmanoglu, M. Braun, R. Hock, F. J. Navarro, Surface velocity and ice discharge of the ice cap on King George Island, Antarctica. *Annals of Glaciology*. **54**, 111–119 (2013).
11. B. Osmanoglu, F. J. Navarro, R. Hock, M. Braun, M. I. Corcuera, Surface velocity and mass balance of Livingston Island ice cap, Antarctica. *Cryosphere*. **8**, 1807–1823 (2014).
- 45 12. M. Minowa, M. Schaefer, S. Sugiyama, D. Sakakibara, P. Skvarca, Frontal ablation and mass loss of the Patagonian icefields. *Earth and Planetary Science Letters*. **561**, 116811 (2021).

13. W. Kochtitzky, L. Copland, W. van Wychen, R. Hugonnet, R. Hock, J. A. Dowdeswell, T. Benham, T. Strozzi, A. Glazovsky, I. Lavrentiev, D. Rounce, R. Millan, A. Cook, A. Dalton, H. Jiskoot, J. Cooley, J. Jania, F. Navarro, Frontal ablation: the unquantified mass loss of marine-terminating glaciers, 2000-2020. *Nature Communications*. **(in press)**.
- 5 14. D. R. Rounce, T. Khurana, M. B. Short, R. Hock, D. E. Shean, D. J. Brinkerhoff, Quantifying parameter uncertainty in a large-scale glacier evolution model using Bayesian inference: Application to High Mountain Asia. *Journal of Glaciology*. **66** (2020), doi:10.1017/jog.2019.91.
- 10 15. D. R. Rounce, R. Hock, D. E. Shean, Glacier Mass Change in High Mountain Asia Through 2100 Using the Open-Source Python Glacier Evolution Model (PyGEM). *Frontiers in Earth Science*. **7** (2020), doi:10.3389/feart.2019.00331.
16. K. Hutter, The Effect of Longitudinal Strain on the Shear Stress of an Ice Sheet: In Defence of Using Stretched Coordinates. *Journal of Glaciology*. **27**, 39–56 (1981).
- 15 17. D. R. Rounce, R. Hock, R. W. McNabb, R. Millan, C. Sommer, M. H. Braun, P. Malz, F. Maussion, J. Mouginot, T. C. Seehaus, D. E. Shean, Distributed Global Debris Thickness Estimates Reveal Debris Significantly Impacts Glacier Mass Balance. *Geophysical Research Letters*. **48** (2021), doi:10.1029/2020GL091311.
- 20 18. D. Farinotti, M. Huss, J. J. Fürst, J. Landmann, H. Machguth, F. Maussion, A. Pandit, A consensus estimate for the ice thickness distribution of all glaciers on Earth. *Nature Geoscience*. **12**, 168–173 (2019).
- 25 19. R. Hock, G. Rasul, C. Adler, B. Cáceres, S. Gruber, Y. Hirabayashi, M. Jackson, A. Käab, S. Kang, S. Kutuzov, A. Milner, U. Molau, S. Morin, B. Orlove, H. Steltzer, "High Mountain Areas" in *IPCC Special Report on the Ocean and Cryosphere in a Changing Climate*, H.-O. Pörtner, D. C. Roberts, V. Masson-Delmotte, P. Zhai, M. Tignor, E. Poloczanska, K. Mintenbeck, A. Alegría, M. Nicolai, A. Okem, J. Petzold, B. Rama, N. M. Weyer, Eds. (2019).
- 30 20. H. Zekollari, M. Huss, D. Farinotti, Modelling the future evolution of glaciers in the European Alps under the EURO-CORDEX RCM ensemble. *Cryosphere*. **13**, 1125–1146 (2019).
21. F. Pithan, T. Mauritsen, Arctic amplification dominated by temperature feedbacks in contemporary climate models. *Nature Geoscience*. **7**, 181–184 (2014).
22. J. Bolibar, A. Rabatel, I. Gouttevin, H. Zekollari, C. Galiez, Nonlinear sensitivity of glacier mass balance to future climate change unveiled by deep learning. *Nature Communications*. **13** (2022), doi:10.1038/s41467-022-28033-0.
- 35 23. RGI Consortium, "Randolph glacier inventory - A dataset of global glacier outlines: Version 6.0" (2017), , doi:10.7265/N5-RGI-60.
24. D. Scherler, H. Wulf, N. Gorelick, Global Assessment of Supraglacial Debris-Cover Extents. *Geophysical Research Letters*. **45**, 11798–11805 (2018).
- 40 25. S. Herreid, F. Pellicciotti, The state of rock debris covering Earth's glaciers. *Nature Geoscience*. **13**, 621–627 (2020).
26. G. Østrem, Ice melting under a thin layer of moraine, and the existence of ice cores in moraine ridges. *Geografiska Annaler*. **41**, 228–230 (1959).
27. D. I. Benn, T. Bolch, K. Hands, J. Gulley, A. Luckman, L. I. Nicholson, D. Quincey, S. Thompson, R. Toumi, S. Wiseman, Response of debris-covered glaciers in the Mount Everest region to recent warming, and implications for outburst flood hazards. *Earth-Science Reviews*. **114** (2012), pp. 156–174.
- 45 28. A. v Rowan, D. L. Egholm, D. J. Quincey, B. Hubbard, O. King, E. S. Miles, K. E. Miles, J. Hornsey, The Role of Differential Ablation and Dynamic Detachment in Driving

Accelerating Mass Loss From a Debris-Covered Himalayan Glacier. *Journal of Geophysical Research: Earth Surface*. **126** (2021), doi:10.1029/2020JF005761.

29. K. B. Tokarska, M. B. Stolpe, S. Sippel, E. M. Fischer, C. J. Smith, F. Lehner, R. Knutti, “Past warming trend constrains future warming in CMIP6 models” (2020), (available at <http://advances.sciencemag.org/>).
30. K. Wyser, E. Kjellström, T. Koenigk, H. Martins, R. Döscher, Warmer climate projections in EC-Earth3-Veg: The role of changes in the greenhouse gas concentrations from CMIP5 to CMIP6. *Environmental Research Letters*. **15** (2020), doi:10.1088/1748-9326/ab81c2.
31. UNEP, “Emissions Gap Report 2021: The Heat is On - A World of Climate Promises Not Yet Delivered” (Nairobi, 2021), (available at <https://www.unep.org/emissions-gap-report-2021>).
32. WGMS, “Fluctuations of Glaciers Database” (Zurich, Switzerland, 2021), , doi:10.5904/wgms-fog-2021-05.
33. H. Hersbach, B. Bell, P. Berrisford, S. Hirahara, A. Horányi, J. Muñoz-Sabater, J. Nicolas, C. Peubey, R. Radu, D. Schepers, A. Simmons, C. Soci, S. Abdalla, X. Abellan, G. Balsamo, P. Bechtold, G. Biavati, J. Bidlot, M. Bonavita, G. de Chiara, P. Dahlgren, D. Dee, M. Diamantakis, R. Dragani, J. Flemming, R. Forbes, M. Fuentes, A. Geer, L. Haimberger, S. Healy, R. J. Hogan, E. Hólm, M. Janisková, S. Keeley, P. Laloyaux, P. Lopez, C. Lupu, G. Radnoti, P. de Rosnay, I. Rozum, F. Vamborg, S. Villaume, J. N. Thépaut, The ERA5 global reanalysis. *Quarterly Journal of the Royal Meteorological Society*. **146**, 1999–2049 (2020).
34. P. A. Arias, N. Bellouin, E. Coppola, R. G. Jones, G. Krinner, J. Marotzke, V. Naik, M. D. Palmer, G.-K. Plattner, J. Rogelj, M. Rojas, J. Sillmann, T. Storelvmo, P. W. Thorne, B. Trewin, K. Achuta Rao, B. Adhikary, R. P. Allan, K. Armour, G. Bala, R. Barimalala, S. Berger, J. G. Canadell, C. Cassou, A. Cherchi, W. Collins, W. D. Collins, S. L. Connors, S. Corti, F. Cruz, F. J. Dentener, C. Dereczynski, A. di Luca, A. Diongue Niang, F. J. Doblas-Reyes, A. Dosio, H. Douville, F. Engelbrecht, V. Eyring, E. Fischer, P. Forster, B. Fox-Kemper, J. S. Fuglestedt, J. C. Fyfe, N. P. Gillet, L. Goldfarb, I. Gorodetskaya, J. M. Gutierrez, R. Hamdi, E. Hawkins, H. T. Heewitt, P. Hope, A. S. Islam, C. Jones, D. S. Kaufman, R. E. Kopp, Y. Kosaka, J. Kossin, S. Krakovska, J.-Y. Lee, J. Li, T. Mauritsen, T. K. Maycock, M. Meinshausen, S.-K. Min, P. M. S. Monteiro, T. Ngo-Duc, F. Otto, I. Pinto, A. Pirani, K. Raghavan, R. Ranasinghe, A. C. Ruane, L. Ruiz, J.-B. Sallée, B. H. Samsat, S. Sathyendranath, S. I. Seneviratne, A. A. Sörensson, S. Szopa, I. Takayabu, A.-M. Trguier, B. van den Hurk, R. Vautard, K. von Schuckmann, S. Zaehle, X. Zhang, K. Zickfeld, "Technical Summary" in *Climate Change 2021: The Physical Science Basis. Contribution of Working Group I to the Sixth Assessment Report of the Intergovernmental Panel on Climate Change*, V. Masson-Delmotte, P. Zhai, A. Pirani, S. L. Connors, C. Péan, S. Berger, N. Caud, Y. Chen, L. Goldfarb, M. I. Gomis, M. Huang, K. Leitzell, E. Lonnoy, J. B. R. Matthews, T. K. Maycock, T. Waterfield, O. Yelekci, R. Yu, B. Zhou, Eds. (Cambridge University Press, 2021).
35. J. Oerlemans, F. M. Nick, A minimal model of a tidewater glacier. *Annals of Glaciology*. **42**, 1–6 (2005).
36. J. G. Cogley, R. Hock, L. A. Rasmussen, A. A. Arendt, A. Bauder, R. J. Braithwaite, P. Jansso, G. Kaser, M. Möller, L. Nicholson, M. Zemp, “Glossary of Glacier Mass Balance and Related Terms” (Paris, 2011).
37. C. E. Rasmussen, C. K. I. Williams, *Gaussian Processes for Machine Learning* (MIT Press, Cambridge, MA, 2006).

38. D. P. Kingma, J. Ba, Adam: A Method for Stochastic Optimization (2014) (available at <http://arxiv.org/abs/1412.6980>).
39. R. J. Braithwaite, Temperature and precipitation climate at the equilibrium-line altitude of glaciers expressed by the degree-day factor for melting snow. *Journal of Glaciology*. **54**, 437–444 (2008).
40. R. Millan, J. Mouginot, A. Rabatel, M. Morlighem, Ice velocity and thickness of the world’s glaciers. *Nature Geoscience*. **15**, 124–129 (2022).
41. B. Recinos, F. Maussion, T. Rothenpieler, B. Marzeion, Impact of frontal ablation on the ice thickness estimation of marine-terminating glaciers in Alaska. *Cryosphere*. **13**, 2657–2672 (2019).

Acknowledgments: This work was supported in part by the high-performance computing and data storage resources operated by the Research Computing Systems Group at the University of Alaska Fairbanks Geophysical Institute. This text reflects only the author’s view and funding agencies are not responsible for any use that may be made of the information it contains.

Funding:

National Aeronautics and Space Administration grant 80NSSC20K1296 (DR, ReHo)

National Aeronautics and Space Administration grant 80NSSC20K1595 (DR, ReHo)

National Aeronautics and Space Administration grant 80NSSC17K0566 (DR, ReHo)

National Aeronautics and Space Administration grant NNX17AB27G (DR, ReHo)

Tula Foundation and Canada Research Chairs (BM)

National Sciences and Engineering Research Council of Canada (BM, LuCo)

Vanier Graduate Scholarship (WK)

Swiss National Science Foundation, project nr. 184634 (RoHu, MH, LoCo, DF)

ArcticNet Network of Centres of Excellence Canada (LuCo)

University of Ottawa, University Research Chair program (LuCo)

European Union’s Horizon 2020 research and innovation programme grant 101003687 (FM)

Austrian Science Fund (FWF) grant P30256 (FM)

French Space Agency CNES, (EB, RoHu)

Author contributions:

Conceptualization: DR, ReHo

Data curation: DR

Formal analysis: DR

Funding acquisition: DR, ReHo, MH, DF, EB, BM, LuCo

Investigation: DR

Methodology: DR, FM, ReHo

Project administration: DR, ReHo

Resources: DR, FM (glacier data); RoHu, MH, EB, DF, BM, and RM (mass balance data); LoCo (climate data); WK and LuCo (frontal ablation data)

Software: DR (PyGEM); FM (OGGM); DB (emulators)

5

Visualization: DR, ReHo

Writing – original draft: DR

Writing – review & editing: all authors, especially ReHo

Competing interests: Authors declare that they have no competing interests.

10

Data and materials availability: The datasets generated for this study can be found in the National Snow & Ice Data Center (NSIDC) following acceptance. During the review process, the data will be publicly available at

<https://drive.google.com/drive/folders/1VXLkBxnj521j6HHy6RUFerqgiZGxMNqG?usp=sharing>. The model code is publicly available at <https://github.com/drounce/PyGEM> and <https://github.com/OGGM/ogggm>.

15

Supplementary Materials

Methods

References (32–41)

Figs. S1 to S28

20

Tables S1 to S5